





# Room-temperature multiferroic behavior in layer-structured Aurivillius phase ceramics

Cite as: Appl. Phys. Lett. **117**, 052903 (2020); <https://doi.org/10.1063/5.0017781>

Submitted: 09 June 2020 . Accepted: 25 July 2020 . Published Online: 07 August 2020

Zheng Li, Vladimir Koval , Amit Mahajan, Zhipeng Gao, Carlo Vecchini, Mark Stewart, Markys G. Cain , Kun Tao, Chenglong Jia , Giuseppe Viola, and Haixue Yan 



View Online



Export Citation



CrossMark

## ARTICLES YOU MAY BE INTERESTED IN

[Intrinsic piezoelectricity in \(K,Na\)NbO<sub>3</sub>-based lead-free single crystal: Piezoelectric anisotropy and its evolution with temperature](#)

Applied Physics Letters **117**, 052904 (2020); <https://doi.org/10.1063/5.0012124>

[Current-induced bulk magnetization of a chiral crystal CrNb<sub>3</sub>S<sub>6</sub>](#)

Applied Physics Letters **117**, 052408 (2020); <https://doi.org/10.1063/5.0017882>

[Magnetic transition behavior and large topological Hall effect in hexagonal Mn<sub>2-x</sub>Fe<sub>1+x</sub>Sn \(x = 0.1\) magnet](#)

Applied Physics Letters **117**, 052407 (2020); <https://doi.org/10.1063/5.0011570>



**Measure Ready**  
**FastHall™ Station**

The highest performance table-top system...  
for Van der Pauw and Hall bar samples

[Learn more](#)

**Lake Shore**  
CRYOTRONICS

# Room-temperature multiferroic behavior in layer-structured Aurivillius phase ceramics

Cite as: Appl. Phys. Lett. **117**, 052903 (2020); doi: [10.1063/5.0017781](https://doi.org/10.1063/5.0017781)

Submitted: 9 June 2020 · Accepted: 25 July 2020 ·

Published Online: 7 August 2020 · Corrected: 11 August 2020



View Online



Export Citation



CrossMark

Zheng Li,<sup>1</sup> Vladimir Koval,<sup>2</sup> Amit Mahajan,<sup>3</sup> Zhipeng Gao,<sup>4</sup> Carlo Vecchini,<sup>5</sup> Mark Stewart,<sup>5</sup> Markys G. Cain,<sup>6</sup> Kun Tao,<sup>7</sup> Chenglong Jia,<sup>7,a)</sup> Giuseppe Viola,<sup>3</sup> and Haixue Yan<sup>3,b)</sup> 

## AFFILIATIONS

<sup>1</sup>Guangdong Provincial Key Laboratory of Applied Superconductivity, Guangdong University of Technology, Guangzhou 510640, China

<sup>2</sup>Department of Materials Science and Engineering, Tsinghua University, Beijing 100084, China

<sup>3</sup>Department of Materials Science and Engineering, University of California, Los Angeles, Los Angeles, California 90095, USA

<sup>4</sup>National Key Laboratory of Materials Physics, Institute of Physics, Chinese Academy of Sciences, Beijing 100871, China

<sup>5</sup>Department of Materials Science and Engineering, University of California, Los Angeles, Los Angeles, California 90095, USA

<sup>6</sup>Department of Materials Science and Engineering, University of California, Los Angeles, Los Angeles, California 90095, USA

<sup>7</sup>Department of Materials Science and Engineering, University of California, Los Angeles, Los Angeles, California 90095, USA

a)Email: [cljia@ucla.edu](mailto:cljia@ucla.edu)

b)Author to whom correspondence should be addressed: [hyan@ucla.edu](mailto:hyan@ucla.edu)

## ABSTRACT

Multiferroic Aurivillius phase (AP) ceramics exhibit room-temperature ferroelectric (FE) and ferromagnetic (FM) behaviors. However, the origin of the room-temperature multiferroic behavior in APs remains unclear. In this work, we study the room-temperature multiferroic behavior in APs with the general formula  $B_{5.25}L_{0.75}F_2C_3O_{18}$  (where  $B = \text{Bi}, \text{Pb}, \text{Ba}, \text{Sr}, \text{Ca}, \text{La}, \text{Pr}, \text{Nd}, \text{Sm}, \text{Eu}, \text{Gd}, \text{Yb}, \text{Lu}$ ;  $L = \text{Ca}, \text{Sr}, \text{Ba}, \text{Pb}, \text{Bi}$ ;  $F = \text{F}, \text{Cl}, \text{Br}, \text{I}$ ;  $C = \text{Fe}, \text{Co}, \text{Ni}, \text{Mn}, \text{Cu}, \text{Zn}, \text{Al}, \text{Ga}, \text{In}, \text{Sn}, \text{Sb}, \text{Bi}, \text{Pb}, \text{Ba}, \text{Sr}, \text{Ca}, \text{La}, \text{Pr}, \text{Nd}, \text{Sm}, \text{Eu}, \text{Gd}, \text{Yb}, \text{Lu}$ ). The room-temperature multiferroic behavior is observed in APs with  $B = \text{Bi}, \text{Pb}, \text{Ba}, \text{Sr}, \text{Ca}, \text{La}, \text{Pr}, \text{Nd}, \text{Sm}, \text{Eu}, \text{Gd}, \text{Yb}, \text{Lu}$  and  $L = \text{Ca}, \text{Sr}, \text{Ba}, \text{Pb}, \text{Bi}$ . The room-temperature multiferroic behavior is attributed to the presence of  $F^{3+}$  and  $C^{3+}$  ions in the AP structure. The room-temperature multiferroic behavior is observed in APs with  $B = \text{Bi}, \text{Pb}, \text{Ba}, \text{Sr}, \text{Ca}, \text{La}, \text{Pr}, \text{Nd}, \text{Sm}, \text{Eu}, \text{Gd}, \text{Yb}, \text{Lu}$  and  $L = \text{Ca}, \text{Sr}, \text{Ba}, \text{Pb}, \text{Bi}$ . The room-temperature multiferroic behavior is attributed to the presence of  $F^{3+}$  and  $C^{3+}$  ions in the AP structure.

Published under license by AIP Publishing. <https://doi.org/10.1063/5.0017781>

Multiferroic Aurivillius phase (AP) ceramics exhibit room-temperature ferroelectric (FE) and ferromagnetic (FM) behaviors. However, the origin of the room-temperature multiferroic behavior in APs remains unclear. In this work, we study the room-temperature multiferroic behavior in APs with the general formula  $B_5F_2C_3O_{18}$  (where  $B = \text{Bi}, \text{Pb}, \text{Ba}, \text{Sr}, \text{Ca}, \text{La}, \text{Pr}, \text{Nd}, \text{Sm}, \text{Eu}, \text{Gd}, \text{Yb}, \text{Lu}$ ;  $L = \text{Ca}, \text{Sr}, \text{Ba}, \text{Pb}, \text{Bi}$ ;  $F = \text{F}, \text{Cl}, \text{Br}, \text{I}$ ;  $C = \text{Fe}, \text{Co}, \text{Ni}, \text{Mn}, \text{Cu}, \text{Zn}, \text{Al}, \text{Ga}, \text{In}, \text{Sn}, \text{Sb}, \text{Bi}, \text{Pb}, \text{Ba}, \text{Sr}, \text{Ca}, \text{La}, \text{Pr}, \text{Nd}, \text{Sm}, \text{Eu}, \text{Gd}, \text{Yb}, \text{Lu}$ ). The room-temperature multiferroic behavior is observed in APs with  $B = \text{Bi}, \text{Pb}, \text{Ba}, \text{Sr}, \text{Ca}, \text{La}, \text{Pr}, \text{Nd}, \text{Sm}, \text{Eu}, \text{Gd}, \text{Yb}, \text{Lu}$  and  $L = \text{Ca}, \text{Sr}, \text{Ba}, \text{Pb}, \text{Bi}$ . The room-temperature multiferroic behavior is attributed to the presence of  $F^{3+}$  and  $C^{3+}$  ions in the AP structure. The room-temperature multiferroic behavior is observed in APs with  $B = \text{Bi}, \text{Pb}, \text{Ba}, \text{Sr}, \text{Ca}, \text{La}, \text{Pr}, \text{Nd}, \text{Sm}, \text{Eu}, \text{Gd}, \text{Yb}, \text{Lu}$  and  $L = \text{Ca}, \text{Sr}, \text{Ba}, \text{Pb}, \text{Bi}$ . The room-temperature multiferroic behavior is attributed to the presence of  $F^{3+}$  and  $C^{3+}$  ions in the AP structure.

$B_{5.25}L_{0.75}F_{1.0}C_{3.0}O_{18}$   
 (BLFC) P L A P  
 F, A C, D  
 $a b$ , P  
 BLFC  
 $a b$  A  
 A *in situ* I H I I  
 N F AL, D, O, U K.  
 (P), A BLFC  
 P  
 BLFC P  
 F 1 (D) BLFC  
 A  
 $B2cb$  A  
 A  $A2_1$   
 $B2cb$   $a = 5.4530(2)$  Å,  $b = 5.4427(1)$  Å,  
 $c = 50.670(2)$  Å  $A2_1am$   $a = 5.4651(6)$  Å,  
 $b = 5.3943(6)$  Å,  $c = 41.487(2)$  Å  
 F P ( // )

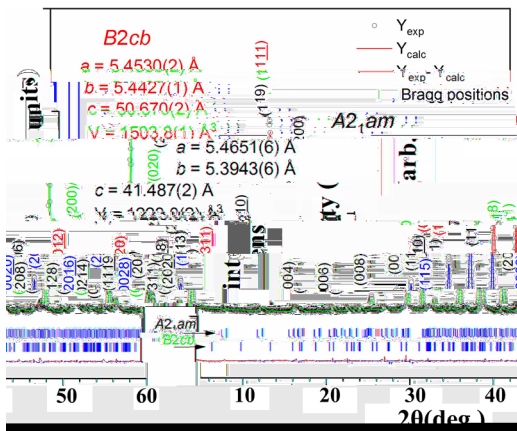


FIG. 1. XRD patterns of B2cb and A2<sub>1</sub>am phases.

BLFC = 4 = 5 A N  
 BLFC F 1 EM (a-b) D  
 P M  
 F 1  
 D. ED 1.4 %, (F 2  
 1)  
 F, C, O, C<sub>2</sub>F O<sub>4</sub>  
 A B<sub>5</sub>F<sub>0.5</sub>C<sub>0.5</sub>O<sub>15</sub><sup>16</sup>  
 BLFC  
 P (50, 70 100,  
 300, 500 H).  
 1060 K FE T BLFC H,  
 ( 973 K).<sup>13</sup> F BLFC P-E I-E B<sub>6</sub> F<sub>3</sub> O<sub>18</sub>  
 BLFC 2( )  
 P BLFC I-E  
 BLFC 21,22  
 BLFC 10 μC/ F 2( )  
 ( FC) (FC) 200 O BLFC BLFC

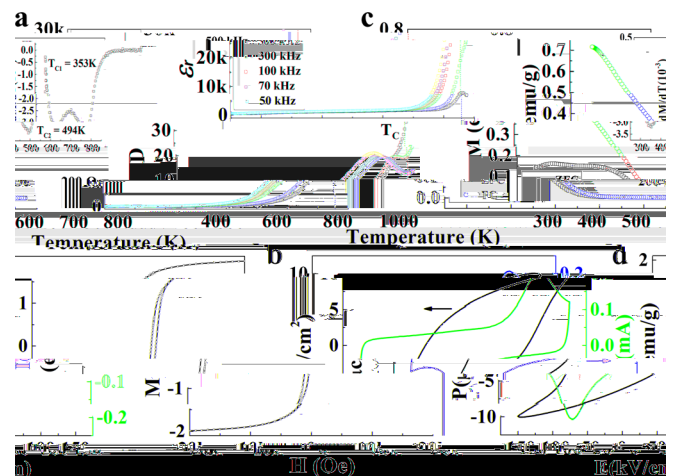


FIG. 2. (a) Temperature dependence of dielectric constant (ε') and dielectric loss (ε'') for BLFC. (b) Temperature dependence of dielectric constant (ε') for BLFC. (c) Temperature dependence of dielectric constant (ε') for BLFC. (d) Temperature dependence of piezoelectric coefficient (d<sub>33</sub>) for BLFC.

( $\sim 494\text{ K}$ ,  $M/$ ),  
 BLFC  $\text{B}_6\text{F C}_3\text{O}_{18}$  (526 K).<sup>23</sup>  
 $\text{F}^{3+} \text{O F}^{3+}, \text{C}^{3+} \text{O C}^{3+}, \text{F}^{3+} \text{O C}^{3+}$  (.  
 ED).<sup>24</sup>  
 A FC  $2 \sim 353\text{ K}$   
 $\text{C}_2\text{F O}_4$   $2$   $\text{C}_2\text{F O}_4$  (460 K)  $16,25$   
 (M)  $\text{C}_2\text{F O}_4$   $0.22 \ 0.32$  / ,  $1.4$  .%  
 $16 \ 23.5$  / .<sup>25</sup> , BLFC  
 $\text{C}_2\text{F O}_4$   $0.22 \ 0.32$  / ,  
 $M = 1.85$  / ,  $F = 2$  ( ) . I  
 $2$  (F . 3).  
 $425\text{ K}$   $1.58$  / .  
 $0.27$  / , ED  
 BLFC  
 A  
 $F = 3$   
 $\text{F}^{3+} \text{O C}^{3+}$   
 (DF ) *ab initio*  
 ( A P) . H  
 $U_F = 2$   $U_C = 3$  F C ,  
 (GGA)  $U$  . I  
 BLFC  
 $F = 3$  ( ) ,  $\text{F}^{3+}$   $\text{C}^{3+}$  (3.1  $2.1 \mu_B$  / , ) ,  
 $0.1 \mu_B$  / ) .  
 $\text{F O}_6$   $\text{C O}_6$   
 F / C -  
 $F$  O - /  $F = 3$  ( ) .  
 $\text{F}^{3+}$   $\text{C}^{3+}$   
 ( . , ) ( . , )  
 $E_{\text{FM}} - E_{\text{AFM}}$   
 $= -144.1$  .  
 H (FM)  
 $43.5$  ( . , 504.6 K),  
 $1$  FC/FC  $F = 2$  ( ) .  
 $a b$   
 010  
 BLFC  $F = 4$  . I  
 PFM BLFC ,  $399\text{ O}$  .  
 $5$  ( ) . A  $F =$   
 F

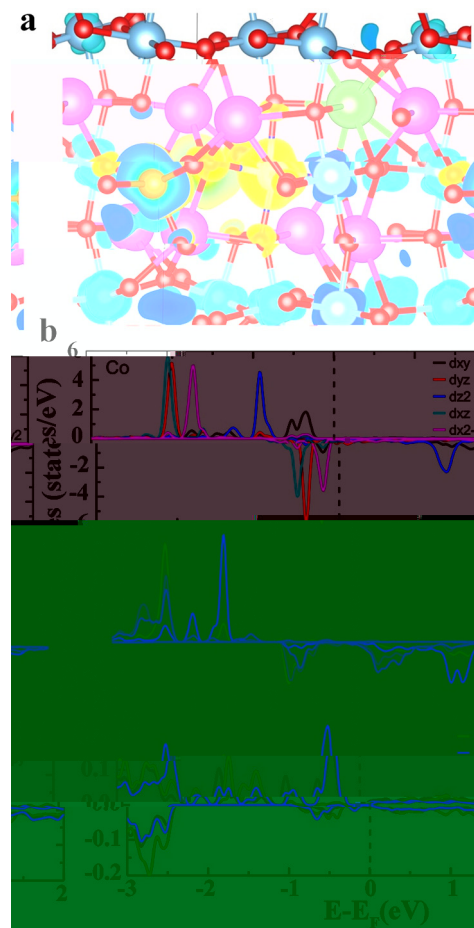


FIG. 3. (a) Crystal structure of BLFC. (b) Density of states (DOS) plot for BLFC showing Co d-orbitals (dxy, dyz, dz2, dxz, dx2y2) and energy in eV.

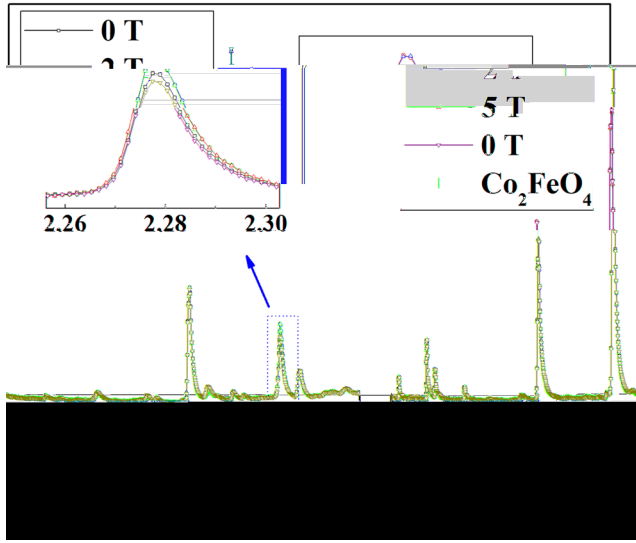


FIG. 4. XRD patterns of  $\text{Co}_2\text{FeO}_4$  at 0 T and 5 T. The inset shows the zoomed-in view of the peak at  $2\theta = 2.28$ .

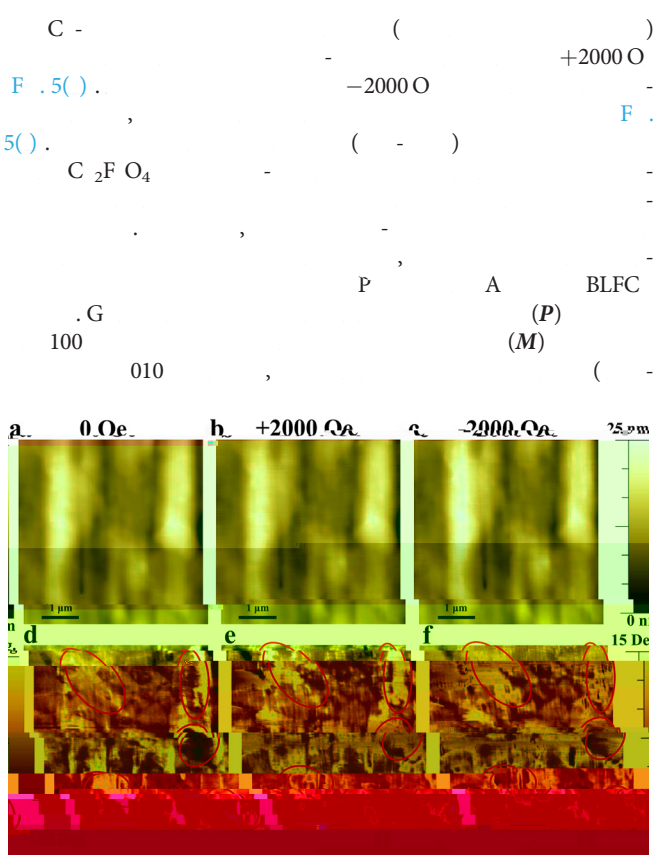


FIG. 5. MFM images of  $\text{Co}_2\text{FeO}_4$  at 0 Oe, +2000 Oe, and -2000 Oe. The top row shows MFM images and the bottom row shows topographic images.

$T = P \times M$   
 BLFC  
 $I = \frac{F}{A}$  BLFC  
 $C^{3+} O C^{3+}, F^{3+} O C^{3+}$   $F^{3+} O F^{3+}$   
 $A, C/F$   
 EM (ED) BLFC  
 D. M, P D. K, D.  
 D I H I I N, AL,  
 D, O K.  
 A E D F  
 G A A (G N. 2/  
 0038/20), C (G N. K2015-0602006), N FC (G  
 N. 11474138 11834005). A  
 E M P (EM)P  
 P IND54 N EM)P  
 EM)P E)AME E

DATA AVAILABILITY

REFERENCES

1. E. N. D. M., J. F., N. 442, 759 (2006).
2. N. A., N. M. 6, 21 (2007).
3. J. M., J. H., L., C. N., A. M. 23, 1062 (2011).
4. L. F. H., O. C., J. B., J. L., C. H., H., O. G., D. C. L., H., K., A. J. B., A. F. M. 26, 2111 (2016).
5. N. A. H., J. P. C. B 104, 6694 (2000).
6. B. A., M. : IL.
7. B. 4 3O12, A. K. I(58), 499 512 (1949).
7. A., G. K., M. M. K., J. P. C. M. 11, 3335 (1999).
8. N. P., G. K., M. E., B 108, 194 (2004).
9. L. K., M., M., A. A., N. D., N. P., M., E. P., D. J., J. A. C. 96, 2339 (2013).
10. L., J. M., G., G., K., A. M., L., C. J., C. N., H., D. 45, 14049 (2016).
11. J. F., NPGA M. 5, 72 (2013).
12. A. B., C. E., P. B 90, 214109 (2014).
13. J. B. L., P. H., G. H., G. L., J. L., J. C., J. K. L., A. P. L. 96, 222903 (2010).
14. M., C., L., A. P. L. 95, 082901 (2009).
15. L., J., L., J. D., A. P. L. 101, 122402 (2012).

- <sup>16</sup>M. P. , P. C. , M. B. , A. P. B. , J. P. H. , K. , L. K. , M. P. , C. , H. K. , A. J. B. , *J. A. P.* **112**, 073919 (2012).
- <sup>17</sup>J. L. , H. , M. J. , K. , P. , *J. A. P.* **102**, 104107 (2007).
- <sup>18</sup>M. G. C. , *Characterisation of Ferroelectric Bulk Materials and Thin Films* ( , 2014), .2.
- <sup>19</sup>.L., K. , J. M. , .G. , .K. , C. J. , G. , H. , A. M. , J. C. , M. C. , I. A. , C. N. , C. J. , H. , *J. M. C. C.* **6**, 2733 (2018).
- <sup>20</sup>.K. , I. , G. , M. , C. J. , H. , *J. P. C.* **122**, 15733 (2018).
- <sup>21</sup>L. J. , F. L. , , *J. A. C.* **97**, 1 (2014).
- <sup>22</sup>H. , F. I. , G. , H. N. , H. , J. , .G. , M. J. , *J. A. D.* **1**, 107 (2011).
- <sup>23</sup>J. , L. , .L. , . , J. D. , . , A. . *P. L.* **101**, 012402 (2012).
- <sup>24</sup>B. , J. , J. C. , .L. , . , J. D. , . , . , *A. P. L.* **104**, 062413 (2014).
- <sup>25</sup>I. P. M. , N. B. , . . . **11**, 719 (2009).